Theory of the local density of surface states on a metal: Comparison with scanning tunneling spectroscopy of a Au(111) surface

L. C. Davis, M. P. Everson, and R. C. Jaklevic
Research Staff, Ford Motor Company, Dearborn, Michigan 48121-2053

Weidian Shen
Science Division, Northeast Missouri State University, Kirksville, Missouri 63501
(Received 27 June 1990)

A simple theory of the effect of monatomic steps on the local density of surface states and on the conductance of a scanning tunneling microscope (STM) has been developed. This theory is based upon reflection and transmission amplitudes for surface electron waves. It is assumed that a step acts as a repulsive barrier, which is entirely consistent with experimental observations on the (111) surface of a Au single crystal. Comparison to experiment has been made for a flat surface to establish that the model for the tip and barrier is adequate. The theory for the conductance with the STM tip near a single step and in the center of a pit is shown to agree well with experiment. Theoretical results are also presented for a periodic array of steps for which one-dimensional Kronig-Penney bands should be observable, especially at reduced temperature.

I. INTRODUCTION

The scanning tunneling microscope (STM) has two distinct attributes: (1) topographical imaging and (2) spectroscopy. The first pertains to the determination of the surface height as a function of location. Features such as monatomic steps[1] and marks made on the surface of metals by a controlled tip touch[2] can be observed easily and even followed as a function of time. The second attribute is the ability to infer information about the surface density of states from the voltage dependence of the current, or the conductance dI/dV. A good example is the surface state on Au(111) observed with the STM by Kaiser and Jaklevic.[3] It is also possible to obtain spectroscopic images of a surface—that is, a scan based upon the value of dI/dV at a fixed voltage related to an electron energy level. This has been demonstrated for semiconductor surfaces by Hamers, Tromp, and Demuth[4] and for metal surfaces by Everson, Jaklevic, and Shen.[5]

To appreciate fully the information from a spectroscopic scan it is useful to analyze a simple, well-characterized sample. A convenient choice is the Shockley-type surface state near the Fermi level on the (111) surface of Au. These states have been studied extensively on Au, Ag, and Cu by photoemission (see Ref. 6 and references therein).

The details of the experimental parts of this work have been described previously.[5,7] Briefly, the experiments are performed in an ultrahigh vacuum on a single-crystal Au(111) surface prepared by ion-bombardment cleaning and thermal annealing. The tunneling tip is usually made from tungsten or platinum. Both topographic and spectroscopic data can be taken simultaneously; the former is taken in the constant current mode where the altitude of the tip is recorded and in the latter the amplitude of the dI/dV (conductance) signal at constant height is taken. Plots of these can be made over the entire scanning area. In addition, complete dI/dV versus tunneling voltage curves may be taken at various points on the surface to measure the position, shape, and intensity of the surface-state peak. These effects are weak, typically about 1% of the background resistance, thus requiring an averaging procedure. Hence, some time is spent at each point on the surface so that repetitive sweeps of the voltage can be made and the resultant conductance can be averaged over 20 to 100 sweeps to achieve adequate signal-to-noise ratio. Semiconductor peaks reported previously,[4] by contrast, have as much as one hundred times greater intensities. For the energy range of interest, the tip voltage is scanned in the positive direction up to 3 V.

In order to have both a good signal-to-noise ratio and small drift during dI/dV acquisition, modulation voltages of 100–200 mV peak to peak were required. The broadening of the surface-state conductance peaks caused by this large modulation voltage must be accounted for when comparing experimental results with theory.

Effects of the Au(111) $23\times\sqrt{3}$ reconstruction[8] have been imaged in these experiments in both topographic and spectroscopic modes.[5] The reconstruction has an effect on the surface-state conductance which is smaller than that measured at a monatomic step (see Sec. III A). Additionally, the magnitude of the surface-state conductance change at a step is independent of whether or not the reconstruction corrugation can be imaged for that particular region. The data suggest that the effect of the reconstruction is only a perturbation of the basic reduction in surface-state conductance measured at a step. Thus we model the Au(111) terraces as flat, even though this is clearly an approximation for reconstructed surface regions.

In Sec. II, we present a simple theory for the current, or dI/dV, as a function of voltage for a band of surface

states on a flat surface and compare to experimental results. Calculations are extended to explore effects due to steps, pits, etc. in Sec. III and to interpret experimental results. Our conclusions are states in Sec. IV.

II. SURFACE-STATE CONDUCTANCE FOR FLAT SURFACE

Kevan and Gaylord[6] measured the dispersion of the surface state as a function of the surface wave vector $\mathbf{k}$. They found that the energy is given by

$$E(\mathbf{k})=E_F-E_0+\hbar^2k^2/2m^* , \tag{1}$$

where E_F is the Fermi energy and for Au $E_0=0.408$ eV and $m^*=0.284m$. Similar states exist on the (111) surface of Cu and Ag. As indicated in Fig. 1(a), this surface band of states exists in a gap in the bulk density of states projected on the (111) surface. Thus a state described by $\mathbf{k}$ has a long lifetime because decay into bulk states is forbidden by momentum conservation.

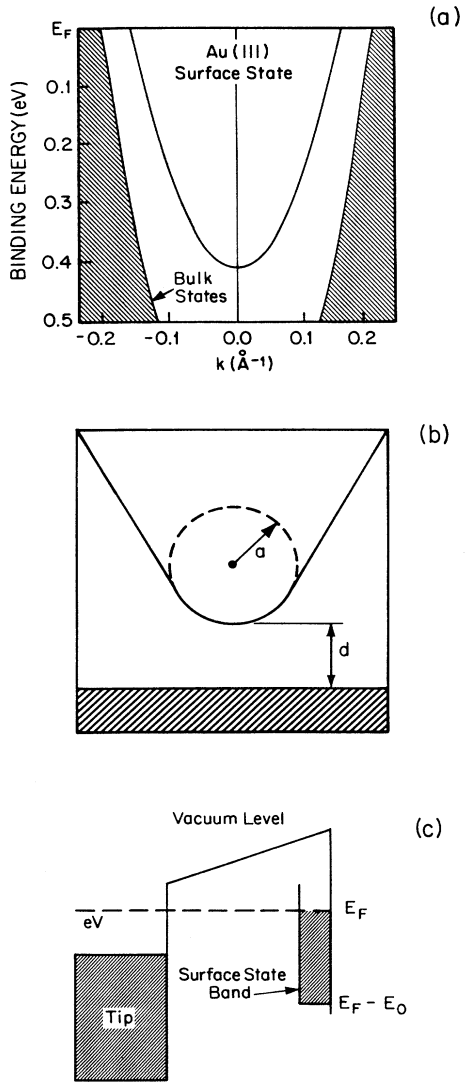

FIG. 1. (a) Surface-state band on Au(111), after Ref. 6. (b) Model of STM tip, after Ref. 9. (c) Energy levels of tip and surface-state band.

In the direction normal to the surface, the state is localized in a wave function that decays into the vacuum as

$$\psi_{\mathbf{k}}(z)\sim e^{i\mathbf{k}\cdot\boldsymbol{\rho}}\exp\left[-\int_0^z K(z)dz\right] , \tag{2a}$$

$$K(z)=\{2m[U(z)-E(\mathbf{k})]/\hbar^2+k^2\}^{1/2} , \tag{2b}$$

where $U(z)$ is the potential and $\boldsymbol{\rho}=(x,y,0)$. For simplicity, we take $U(z)=\Phi+E_F-eV/2$, where V is the potential on the tip and Φ is the work function of the Au(111) surface.

Following Tersoff and Hamman,[9] we approximate the μth tip wave function as (the s-wave approximation)

$$\psi_\mu(r)\sim e^{-\kappa(r-a)}/r , \tag{3a}$$

$$\kappa=[2m(-E_\mu-eV/2)/\hbar^2]^{1/2} , \tag{3b}$$

$$r=[x^2+y^2+(z-z_0)^2]^{1/2} , \tag{3c}$$

where a is the tip radius of curvature, $z_0=d+a$, and d is the distance from the Au surface to the tip [Fig. 1(b)].

Since the surface state is not propagating in the z direction, it is appropriate to use the Bardeen formalism[10] to calculate the current. The assumption is that an electron injected into an unoccupied surface state (negative bias V) propagates laterally away from the tip or thermalizes before it can tunnel back into the tip. Likewise, it is assumed that an electron removed from a surface state (positive bias) goes into a continuum of tip states and does not tunnel back into the Au [Fig. 1(c)]. The current is

$$I=\frac{2\pi e}{\hbar}\sum_{\mu,\nu}[f(E_\nu)-f(E_\mu+eV)]|M_{\mu\nu}|^2\delta(E_\mu-E_\nu) , \tag{4a}$$

$$M_{\mu\nu}=\frac{\hbar^2}{2m}\int d\mathbf{S}\cdot(\psi_\mu^*\nabla\psi_\nu-\psi_\nu\nabla\psi_\mu^*) , \tag{4b}$$

where ν stands for $\mathbf{k}$, $f(E)$ is the Fermi function, and the $d\mathbf{S}$ integration is over any surface between the tip and the Au surface. Hence (for $k\ll\kappa$)

$$M\sim\exp\left[-\int_0^d K(z)dz-\frac{ak^2}{2\kappa}\right] , \tag{5}$$

where we have made use of an expansion of the tip wave function in Fourier components in the plane $z=d$ [see Eqs. (6) and (7) of Ref. 9]. Although we use Eq. (5) to describe the effect of the tip radius of curvature, we do not vary a in our calculations because the results may not be significant. For instance, a blunt tip would correspond to large a. However, in this limit one could treat the tip as a planar surface for which the matrix would be given, paradoxically, by Eq. (5) with $a=0$. Higher-l wave functions have weaker dependence on k due to the radius of curvature than s waves. Hence, the s-wave approximation breaks down for a blunt tip. Presumably, Eq. (5) holds

over a limited range that is relevant to sharp tips. [For further discussion of the validity and limitations of the approximate tip function (3), see Refs. 11, 12, 13, 14, and 15. If the tip wave function were a d_{z^2} function as suggested by Chen,[15] the modification of the results, in particular, Eq. (5), is insignificant.] Substituting (5) into Eq. (4a), we have

$$I \sim \int_0^\infty dE \exp\left[-2\int_0^d K(z)dz - \frac{E}{E_a}\right] \times [f(E_F - E_0 + E) - f(E_F - E_0 + E + eV)] , \quad (6a)$$

$$E = \frac{\hbar^2 k^2}{2m^*} , \quad (6b)$$

$$E_a = \frac{\hbar^2 \kappa}{2m^* a} . \quad (6c)$$

In principle, the tip density of states should appear in (6a). However, since we have no knowledge of its energy dependence, we treat it as a constant.

For a qualitative understanding, we can expand $\int K(z)dz$ for small V and E to obtain the simplified expression

$$I = G_0 \exp(V/V_0) \times \int_0^\infty dE \exp[(E_0 - E)/E_1] \times [f(E_F - E_0 + E) - f(E_F - E_0 + E + eV)] , \quad (7a)$$

$$V_0 = \frac{2(\hbar^2 \Phi / 2m)^{1/2}}{ed} , \quad (7b)$$

$$E_1 = E_a / [1 + d(1 - m/m^*)/a] , \quad (7c)$$

where G_0 is the surface-state conductance at zero bias and $T=0$.

A typical result of this theory is shown in Fig. 2 where we plot the conductance (in units of G_0) for two different temperatures. In the numerical calculations, we use the more accurate form (6), instead of (7). For low T (essentially $T=0$), the conductance is just the surface-state density of states (DOS) distorted by the voltage and E dependences of the tunneling probability. Recall that the DOS for 2D free electrons is uniform above the bottom of the band at $E_F - E_0$ [Fig. 1(c)]. At room temperature, where all the experiments discussed in this paper were performed, the discontinuous change in dI/dV at $V = E_0/e$ that occurs at $T=0$ is smeared out giving the appearance of a peak. The position of the peak depends on T and is always less than E_0/e. For the parameters chosen ($a=20$ Å, $d=9$ Å, $\Phi=4$ eV, and $T=300$ K), the peak occurs at 0.34 V. Two typical experimental conductance curves are displayed in Fig. 3. Since the assignment of background (due to bulk states) is not unambiguous, it is difficult to normalize the spectra. Here, for comparison to theory, we have normalized the difference in conductance between the peak and the subsequent minimum to the theoretical value. The calculated curve shown in Fig. 3 is the 300-K curve of Fig. 2, which has been broadened to account for the 200-mV (peak-to-peak) modulation used in the experiment and has had a linear background term added. It is clear that the general shape and location of the experimental peaks agree well with theory. The calculated peak position (with modulation and background), at 0.31 V, compares favorably with experiment. Results from 24 trails spanning many different large (111) terraces give an average peak position of 0.317 V with a standard deviation of 0.043 V. However, the calculated minimum (0.54 V) differs somewhat from the observed values—0.62 to 0.64 V for the examples shown in Fig. 2.

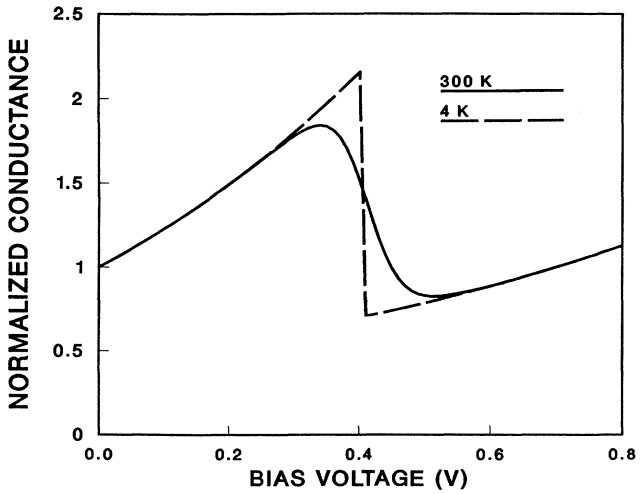

FIG. 2. Surface-state conductance, dI/dV vs V, normalized to unity at zero bias voltage. Solid curve, $T=300$ K; dashed curve, $T=4$ K.

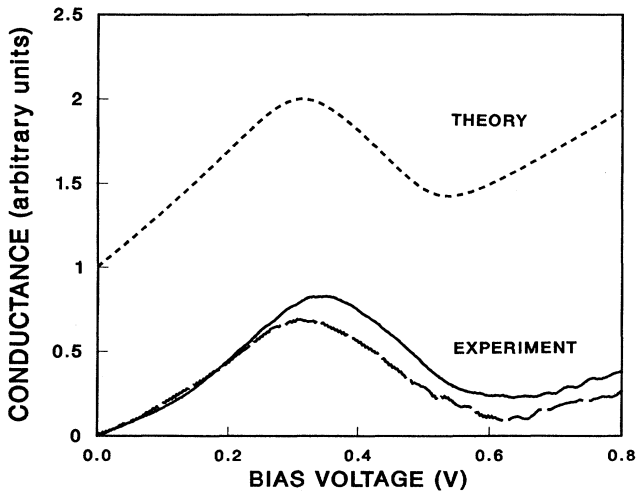

FIG. 3. Conductance dI/dV vs bias voltage V. Solid and long dashed curves are typical experimental results at room temperature where the peak to minimum difference has been normalized to the calculated value. The curves have been offset by one unit for clarity. The short dashed curve is the calculated curve of Fig. 2 for $T=300$ K, which has been broadened to account for the 200-mV modulation in the experiment and has had a linear background added.

One possible explanation for the difference is the effect of the electric field on the energies of the surface states. The field is V/d directly below the tip and, from perturbation theory, would be expected to produce a shift of approximately $-eV/2Kd$. For typical parameters, this shift is of order 0.02 eV and could explain the small differences in the peak voltage between theory and experiment. The position of the minimum is more sensitive to background and is not thought to be as significant as the peak.

Qualitatively similar results for the surface-state conductance have been calculated by Modinos, Aers, and Paranjape[16] in metal-insulator-metal tunneling. They included lifetime broadening, but restricted their calculation to $T=0$.

III. EFFECTS OF SURFACE STRUCTURE

In this section we consider the effects of surface structure on the surface-state energies and tunneling conductance, especially as a function of lateral position. We limit our attention to a single monatomic step, periodically spaced steps, and to isolated pits, which are easily formed on the Au(111) surface and show interesting effects. We are not concerned with the direction of the step because, experimentally, results for different directions are indistinguishable.

The approach used for this analysis assumes that the perturbation due to a step is confined to the immediate vicinity of the step. That is, in the region between (or away from) the steps, the surface electron travels freely (in two dimensions). From the work of Thompson and Huntington,[17] who have calculated the potential near a step in a jellium model, it appears that the principal distortions of the potential occur over a range of a few angstroms on either side of the step. This assumption of a local perturbation then leads to the notion of reflection and transmission of an electron wave impinging on the step (see inset on Fig. 4). If we neglect any coupling to bulk states, then we can define a transmission coefficient T and a reflection coefficient R for an electron impinging normally on a step at the origin:

$$\psi(x)=\begin{cases} e^{-iqx}+Re^{iqx}, & x>0 \quad (8a)\\ Te^{-iqx}, & x<0 \quad (8b)\end{cases}.$$

Conservation of flux requires that $|T|^2+|R|^2=1$. Time-reversal symmetry then demands that an electron impinging on a step from the left [Eq. (8) corresponds to an electron coming from the right] must have the same transmission coefficient T and the same magnitude of reflection coefficient $|R|$, although the phase of the reflection coefficient could be different. It must, however, satisfy $R'=-R^*T/T^*$. Throughout this paper, we assume that $R'=R$.

A. Single step

In this subsection we calculate the conductance for the tip near a single step of height s. Since the surface is translationally invariant in the y direction (parallel to the step), the wave function will have an $\exp(ik_y y)$ dependence. The total wave function is then

$$\Psi(\mathbf{x})=\exp(ik_y y)\psi(x)\Phi(z-\xi)\ , \quad (9a)$$

where

$$\xi=\begin{cases} s, & x<0 \quad (9b)\\ 0, & x>0\ , \quad (9c)\end{cases}$$

and $\psi(x)$ is given by Eq. (8) for an electron impinging on the step from the right. A similar expression holds for an electron impinging from the left. The nature of $\Phi(z)$ is discussed by Kevan and Gaylord[6] and by Zangwill.[18] Its detailed form is not of interest here, except that it decays as $\exp(-Kz)$ into the vacuum. The energy of the state given by Eq. (9) is (relative to the bottom of the surface-state band)

$$E=\hbar^2(q^2+k_y^2)/2m^*\ . \quad (10)$$

The tip wave function is given by Eqs. (3a) and (3b), but with r referred to a tip at position $(x_0,0,z_0)$:

$$r=[(x-x_0)^2+y^2+(z-z_0)^2]^{1/2}\ . \quad (11)$$

The primary dependence of the tip wave function on position is given by expanding r and $\psi_\mu(r)$ about the apex at the tip $(x_0,0,z_0-a)$ on the plane $z=z_0-a$:

$$r\approx a-[(x-x_0)^2+y^2]/2a \quad (12)$$

and

$$\psi_\mu(r)\sim(\kappa/2\pi a)\exp\{-\kappa[(x-x_0)^2+y^2]\}\ . \quad (13)$$

(This approximation gives the same results for small k^2 as obtained by using the expansion of Ref. 9. The normalization is chosen for convenience.) The dominant fac-

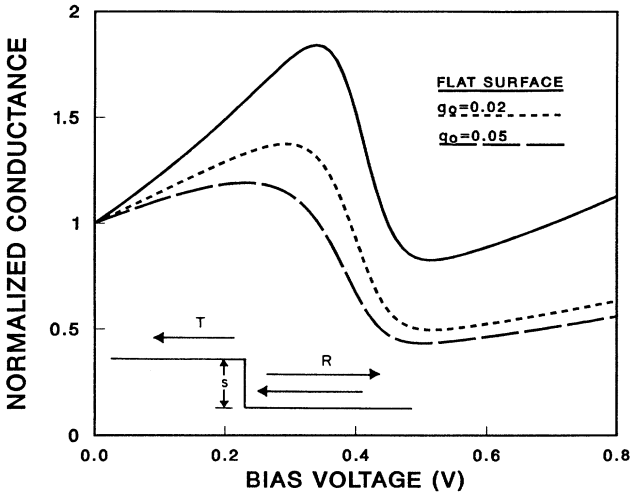

FIG. 4. Normalized conductance vs bias voltage with tip directly over monatomic step. Solid curve, $q_0=0$ (same as flat surface); short dashed curve, $q_0=0.02$ Å^{-1}, long dashed curve, $q_0=0.05$ Å^{-1}. $T=300$ K. Inset: monoatomic step of height s. Surface plane wave impinging normally from the right has a reflection amplitude R and a transmitted amplitude T.

tor in the matrix element (4b) is a surface integral (on the $z=z_0-a=d$ plane) of $\psi_\mu(r)$, as written in Eq. (12), and $\Psi(\mathbf{x})$ from Eq. (9). The y portion of the integral is

$$\sqrt{\kappa/2\pi a}\int_{-\infty}^{\infty} dy\ \exp(ik_y y-\kappa y^2/2a)=\exp(-k_y^2 a/2\kappa)\ . \tag{14}$$

The x portion for an electron impinging from the left involves the following factor:

$$I_L=\int_{-\infty}^{0} dx\ e^{Ks}(e^{iqx}+\mathrm{Re}^{-iqx})(\kappa/2\pi a)^{1/2} \times\exp[-\kappa(x-x_0)^2/2a] + \int_0^{\infty} dx\ Te^{iqx}(\kappa/2\pi a)^{1/2}\exp[-\kappa(x-x_0)^2/2a]. \tag{15}$$

A similar factor I_R is obtained for an electron impinging on the step from the right. The current is

$$I\sim\int_0^{\infty} dk_y\int_0^{\infty} dq\ \exp(-2Kd-k_y^2 a/\kappa)(|I_L|^2+|I_R|^2) \times[f(E_F-E_0+E) -f(E_F-E_0+E+eV)]\ . \tag{16}$$

For $x_0\to\infty$, this expression goes to Eq. (6a), aside from multiplicative constants.

As this point, we must introduce a functional form for the transmission and reflection coefficients. We shall think of the electron attempting to go across the step as tunneling through an effective barrier. For simplicity, we take that barrier to be $U_0 s\delta(x)$. Borland[19] showed that one can always replace a barrier potential by a suitably chosen δ function, although the strength U_0 depends on the energy E. Since we are primarily interested in a small energy range, taking U_0 as constant should be a good approximation. The resulting coefficients are

$$T=q/(q+iq_0) \tag{17}$$

and

$$R=-iq_0/q+iq_0), \tag{18}$$

where

$$q_0=m^*U_0 s/\hbar^2\ . \tag{19}$$

This is the simplest form that a tunneling barrier can take, involving only one adjustable parameter q_0. In the long-wavelength limit ($q\to 0$), common barrier potentials give the forms (17) and (18). Further justification for this approach is given in the Appendix.

In Fig. 4 the calculated, normalized conductance (dI/dV divided by its value at $V=0$) is shown for the tip just above the step ($x_0=0$). The results pertaining to two values of the parameter q_0, 0.02 and 0.05 Å^{-1}, are displayed. These values correspond to $U_0=0.23$ and 0.58 eV, respectively, for $s=2.31$ Å. The conductance above 0.3 V is substantially reduced compared to the flat surface. The energy at which $|T|^2=\frac{1}{2}$, namely, $\hbar^2 q_0^2/2m^*$, is remarkably small, 0.005 and 0.034 eV above the bottom of the surface-state band for the two values chosen. At the Fermi level, the reflectivity $|R|^2$ has dropped to 0.013 and 0.076, respectively—rather weak scattering, yet this order of magnitude for q_0 appears to reproduce the experimental results shown in Fig. 5 reasonably well. The experimental conductance curves could also be affected by a broadening due to coupling (induced by the step potential) of the surface states to the bulk continuum states, which is not included in our calculations. We do not believe that such a broadening would be strongly dependent on position and, therefore, could not explain the observed variation of the conduc-

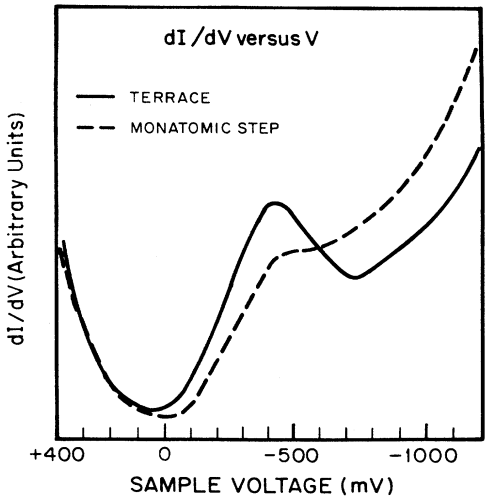

FIG. 5. Experimental conductance vs sample voltage at room temperature. Solid curve, flat surface; dashed curve, same tip positioned over isolated monatomic step. The tip resolution of ~10 Å causes steps to be rounded. For this case the tip was positioned half way (in Δz) up the step profile.

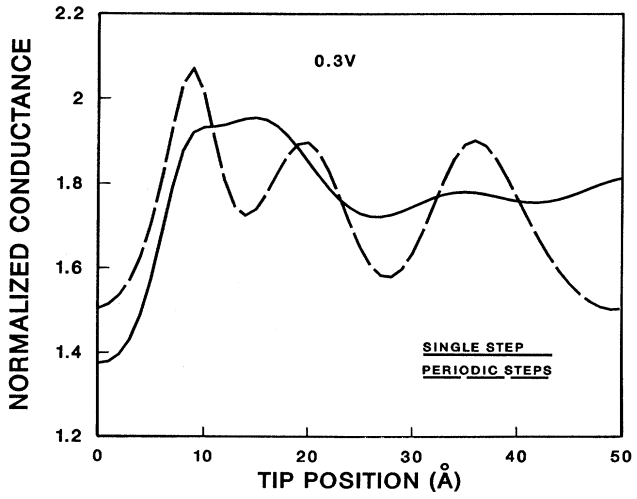

FIG. 6. Normalized conductance dI/dV at 0.3 V vs distance x_0 of the tip from the step. At each x_0, dI/dV at 0 V is set equal to unity. $q_0=0.02$ Å^{-1}, $T=300$ K. Solid curve, single monatomic step; dashed curve, periodic array of monatomic steps spaced 50 Å apart.

tance with position.[5] A calculation of the normalized conductance at $V=0.3$ V as a function of tip position x_0 is shown in Fig. 6 for $q_0=0.02$ Å^{-1}. Also shown is a similar curve where the tip moves between steps in a periodic array (to be discussed in Sec. III B). In both cases, after an initial rise near the step, oscillatory behavior reminiscent of Freidel oscillations occurs.

B. Periodic array of steps

In this subsection the conductance for an array of steps is determined. Let us first calculate the surface-state energies for a periodic array of monatomic steps, equally spaced a distance L apart. Since the surface is periodic in the x direction (one step is the same as another), the wave function must obey Bloch's theorem:

$$\psi(x+L)=\exp(ik_xL)\psi(x) . \tag{20}$$

In the region between the steps at 0 and L, the wave function can be written as

$$\psi(x)=Ae^{iqx}+Be^{-iqx} . \tag{21}$$

In any other region, $\psi(x)$ can be determined by Eq. (20). Note that, in general, q and k_x differ. Applying matching conditions such as Eq. (8) to the step at L, we find

$$Be^{-iqL}=T\exp(ik_xL)B+RAe^{iqL} , \tag{22a}$$

$$A\exp(ik_xL)=TAe^{iqL}+R\exp(ik_xL)B . \tag{22b}$$

Since $q=(2m^*E_x)^{1/2}/\hbar$ (the energy is $E=E_x+\hbar^2k_y^2/2m^*$), the solution of Eq. (22) gives the dispersion relation $E_x(k_x)$ for motion in the x direction:

$$\cos(qL+\phi)=|T|\cos k_xL , \tag{23}$$

or in terms of energy,

$$E_x(k_x)=\frac{\hbar^2}{2m^*L^2}[\cos^{-1}(|T|\cos k_xL)-\phi]^2 , \tag{24}$$

where we have written $T=|T|e^{i\phi}$. Likewise, the coefficients A and B can be determined from Eq. (22) and the normalization.

The dispersion curve $E_x(k_x)$ computed from Eq. (24) has the behavior expected of a 1D Kronig-Penney model. It is also useful to calculate the two-dimensional local density of states for later comparison to the conductance. Taking account of the motion in the y direction, we must evaluate

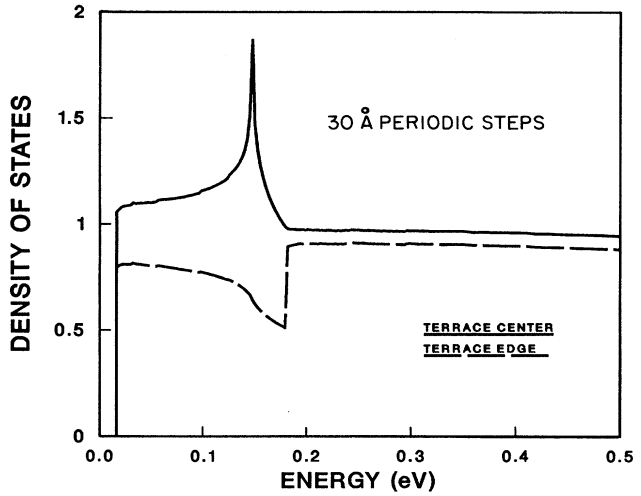

FIG. 7. Local density of states for periodic array of monatomic steps spaced 30 Å apart in units of the flat-surface density of states. Solid curve, midway between steps; dashed curve, immediately over step. $q_0=0.02$ Å^{-1}.

$$n(x,E)=\frac{(2m^*)^{1/2}}{\pi h}\int_0^{k_x(E)}|\psi_{kx}(x)|^2\times[E-E_x(k_x)]^{-1/2}dk_x , \tag{25}$$

where $k_x(E)$ is defined as the value of k_x in the extended zone scheme that satisfies $E_x(k_x)=E$. $\psi_{kx}(x)$, given by Eq. (21), implicitly depends on k_x through q and the relationship (23). A typical local density of states (LDOS) is shown in Fig. 7 ($q_0=0.02$ Å^{-1} and $L=30$ Å). For comparison, the units are chosen such that the flat surface LDOS is unity (independent of x) for $E>0$. As expected for a repulsive step potential, the LDOS at the midpoint exceeds that near the steps. The small gap (0.03 eV) which opens up at $k_x=\pi/L$ ($\hbar^2\pi^2/2m^*L^2=0.15$ eV) is clearly visible. In a separate calculation (not shown), we find that the oscillatory behavior (as a function of tip position) of the conductance at fixed voltage noted in Fig. 6 is a distorted version of oscillations in $n(x,E)$ with x varying and E fixed. It can be shown that in the limit $a=0$, $T=0$, and $\Phi\rightarrow\infty$, the conductance is proportional to the LDOS at $E=E_F-eV$, as Fig. 1(c) suggests.

The current for the stepped surface is obtained in a manner similar to the evaluation for a single step, except that we use the expansion of the tip wave function of Ref. 7 and the relevant surface for the $d\mathbf{S}$ integration in Eq. (4b) is a plane tilted at an angle $\theta=\tan^{-1}(s/L)$ with respect to the xy plane. The result is

$$I\sim\int d^2k[f(E_F-E_0+E)-f(E_f-E_0+E+eV)]e^{-2Kd}\times\left|\sum_n\exp\{-[\cos^2\theta(k_x+G_n)^2+k_y^2]^2a/2\kappa+i(k_x+G_n)(x_0-a\sin\theta)\}\times[AF(Ks,(q-k_x-G_n)L)+BF(Ks,-(q+k_x+G_n)L)]\right|^2 , \tag{26}$$

where

$$G_n = 2\pi n / L \tag{27}$$

and

$$F(u,v) = (e^{u+iv} - 1)/(iu - v) \, . \tag{28}$$

The normalized conductance curves with the tip at the midpoint (terrace center) and over a step (terrace edge) are shown in Fig. 8(a) for $T = 300$ K ($q_0 = 0.02$ Å^{-1}, $L = 30$ Å). The conductance with the tip placed over the step is nearly the same for the array of steps as for a single step (Fig. 4), whereas the conductance at the midpoint is increased and shifted towards zero bias relative to the flat surface. At lower temperature ($T = 77$ K), effects of the gap in the LDOS are evident [Fig. 8(b)]. An observation of these features in a low-temperature experiment would constitute an important verification of the theory. (Note that the effect of a finite mean free path, which has been omitted from the theory, may obscure such an observation.) At present, the data at room temperature are too preliminary to present and do not exist for lower T.

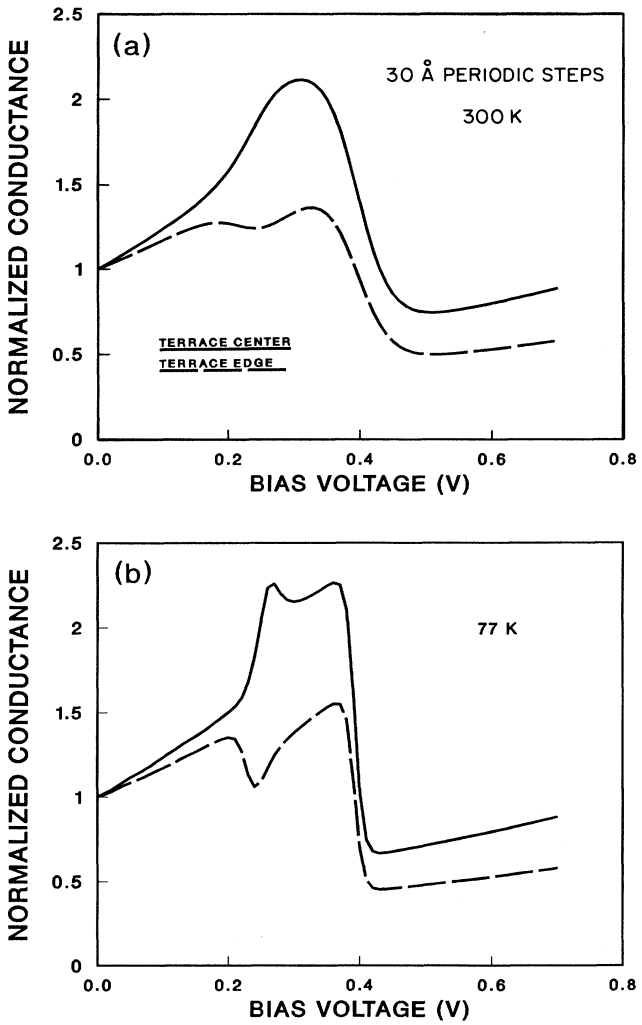

FIG. 8. (a) Normalized conductance vs bias voltage for periodic array of steps in Fig. 7. $T = 300$ K, $q_0 = 0.02$ Å^{-1}. Solid curve, tip positioned midway between steps; dashed curve, tip positioned over step. (b) Same as (a) except $T = 77$ K.

C. Pit

As a further test of the theory, these concepts can also be applied to monatomic pits which can often be found after sputtering the Au(111) surface. Although the actual shape of the perimeter is polygonal due to crystallographic effects, for simplicity we approximate it as a circle of radius R. In the s-wave approximation, only pit states with s-wave symmetry will be involved in the tunneling

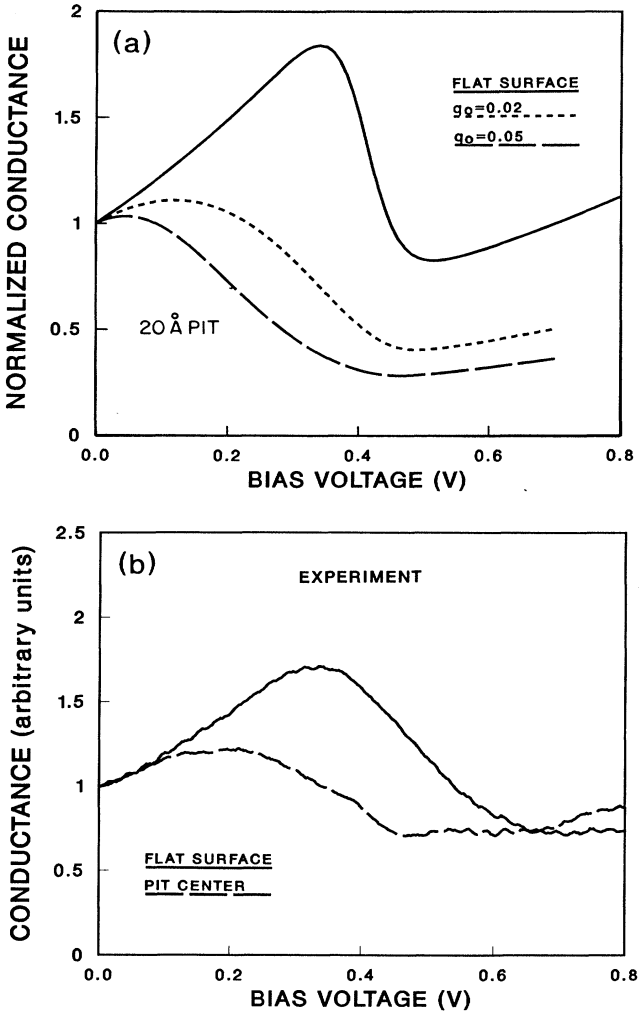

FIG. 9. (a) Normalized conductance vs bias voltage for a 20-Å-diam. pit, one atomic layer deep, tip positioned at center of pit. $T = 300$ K. Solid curve $q_0 = 0$ (flat surface); short dashed curve, $q_0 = 0.02$ Å^{-1}; long dashed curve, $q_0 = 0.05$ Å^{-1}. (b) Experimental conductance vs bias voltage for a 19-Å-diam. pit at room temperature. Dashed curve, tip over center of pit; solid curve, flat surface with same tip. Scale for conductance is the same for both curves which have been vertically aligned at zero bias.

current if the tip is located over the center, which is the only case we consider. Within the pit, the wave function is proportional to a zero-order Bessel function:

$$\psi(\rho)=C(k)J_0(k\rho) . \tag{29}$$

Matching at the boundary $\rho=R$ to a linear combination of $J_0(k\rho)$ and $N_0(k\rho)$ and representing the effective potential at the step as $U_0 s\delta(\rho-R)$, we find

$$C^2(k)=\tfrac{1}{2}k/\{[1-\pi q_0 R J_0(kR)N_0(kR)]^2 + [\pi q_0 R J_0^2(kR)]^2\} . \tag{30}$$

The local density of states is ($E=\hbar^2k^2/2m^*>0$)

$$n(\rho=0,E)=m^*C^2(k)/\pi\hbar^2k . \tag{31}$$

The total wave function is

$$\Psi(\rho,z)=\psi(\rho)\Phi(z-\xi) , \tag{32a}$$

where

$$\xi=\begin{cases} s, & \rho>R \\ 0, & \rho<R \end{cases} . \tag{32b}$$

The matrix element (4b) for the pit wave function contains the surface integral

$$I_P=\int_0^\infty \rho\, d\rho(\kappa/a)\exp(-\rho^2\kappa/2a)\Psi(\rho,d) . \tag{33}$$

If $R^2\gg 2as$,

$$I_P\approx C(k)\exp(-k^2a/2\kappa)e^{-Kd} . \tag{34}$$

The current is

$$I\sim\int_0^\infty dk\, I_P^2[f(E_F-E_0+E)-f(E_F-E_0+E+eV)] . \tag{35}$$

In Fig. 9(a) the normalized conductance is presented

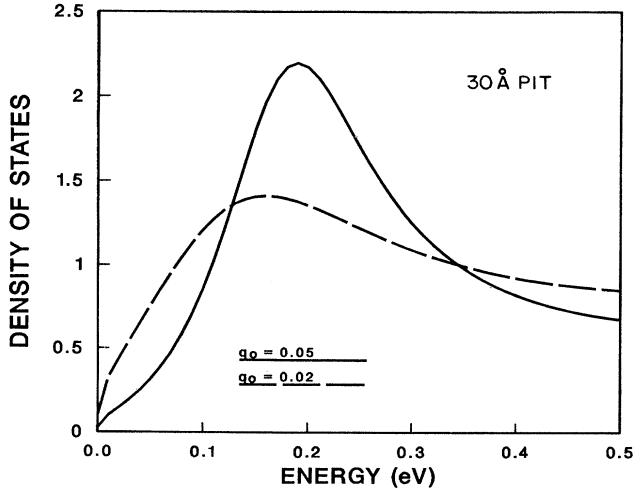

FIG. 10. Density of states at the center of a 30-Å-diam. pit in units of the flat-surface density of states. Solid curve, $q_0=0.05$ Å^{-1}; dashed curve, $q_0=0.02$ Å^{-1}.

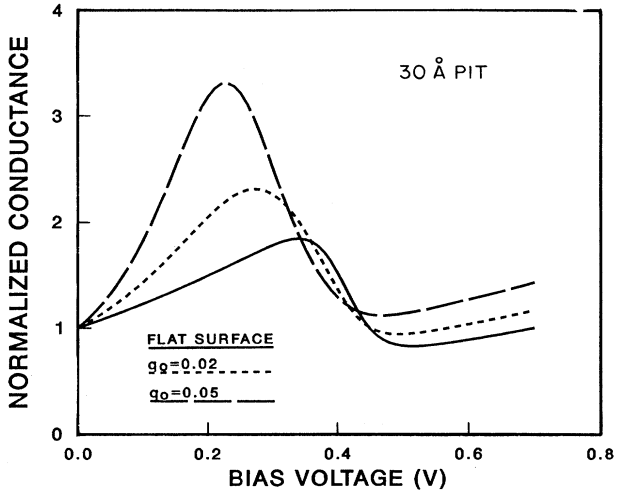

FIG. 11. Normalized conductance vs bias voltage for a 30-Å-diam. pit with tip positioned at center if pit. $T=300$ K. Solid curve, $q_0=0$ (flat surface); short dashed curve, $q_0=0.02$ Å^{-1}; long dashed curve, $q_0=0.05$ Å^{-1}.

for a small pit ($R=10$ Å). The reduction at the center of the pit relative to the flat surface is substantially greater than for either the single step or an array of steps with the tip positioned over a step. The qualitative agreement with experimental data in Fig. 9(b) is good.

For a larger pit ($R=15$ Å), the first resonance of the pit can fall below E_F as indicated in Fig. 10. Only for the stronger scattering ($q_0=0.05$ Å^{-1}) is the resonance fairly well developed. Consequently, the conductance (Fig. 11) shows a large peak which is shifted toward the Fermi level. Preliminary experiments on three different sputter pits of approximately 15 Å radius all show significant shifts of the peak to lower voltage. The average shift in peak position with respect to values for nearby large planar regions is 113 mV, about the size of the shift calculated for $q_0=0.02$ Å^{-1}, as shown in Fig. 11. Significant peak size enhancements have not been observed for these pits.

IV. CONCLUSIONS

The most significant result of this paper is that we have demonstrated that, at least for Au(111), a monatomic step can be treated as a repulsive barrier for free-electron-like, two-dimensional surface states. There is no experimental evidence that steps have an attractive potential or bind surface-state electrons in their vicinity. This is in contrast to a simple model of the surface phonons on fcc (111), where modes localized near a step are found.[20] We have made plausible a simple form for the transmission and reflection amplitudes and have found that a step weakly reflects electrons at the Fermi level. Only within ~10 mV of the bottom of the surface-state band (408 mV below E_F in Au) does the reflection coefficient become significant. From our comparison of experiment to theory, we have been able to extract a parameter $q_0\approx 0.02$ Å^{-1} that measures the strength of the

barrier. This experimentally determined quantity could be compared to more detailed calculations of the surface electronic structure near a step.

Experiments on small pits can be explained using the same description of the repulsive barrier as appropriate for a single step. The conductance with the tip over the pit center is decreased for small pits (e.g., 20 Å diameter), but should be increased for larger pits where the first resonance can occur below E_F.

Theoretical results also indicate that interesting effects due to 1D Kronig-Penney bands can be observed on a surface consisting of a periodic array of steps. To observe such effects clearly, it will probably be necessary to go to low temperatures to escape thermal broadening of the spectra. In general, we find that at room temperature the conductance resembles the local density of surface states, but with considerable broadening. At low temperature, the similarity is much stronger but the energy and voltage dependences of the tunneling still cause the conductance to be a distorted version of the LDOS.

Shapiro, Muller, and Chiang[21] have measured the surface-state dispersion (E vs $\mathbf{k}$) on a stepped surface of Cu, namely, the (332) surface which is tilted 10° from (111) and consists of terraces spaced about 12 Å apart. Using angle-resolved photoemission, they found that the minimum in the dispersion occurred at the zone boundary and not at the center (Γ) as found on a flat (111) surface. Based upon the analysis given in Sec. III B, we would expect the minimum to fall at Γ for wide terraces, suggesting that the potential changes substantially when the steps are close enough to interact.

ACKNOWLEDGMENTS

The authors would like to thank L. Elie for technical assistance and C. B. Duke, M. F. Thorpe, and D. Tomanek for useful discussions.

APPENDIX

In this appendix we attempt to make the form of T, Eq. (17), plausible. For a step with a potential that varies in the x direction as

$$U(x,z)-U(x,z-\xi(x)) ,$$

where $\xi(x)$ varies from 0 to s, we can write the wave function as

$$\Psi(x,z)=\psi(x)\Phi(z-\xi(x)) . \tag{A1}$$

Schrödinger's equation can then be written as

$$\frac{-\hbar^2}{2m^*}\frac{d^2}{dx^2}\psi+U_{\text{eff}}(x)\psi=E\psi , \tag{A2}$$

where the effective potential is

$$U_{\text{eff}}(x)=[\hbar\xi'(x)]^2/2m^*\int_{-\infty}^{\infty}dx[d\Phi(z)/dz]^2 . \tag{A3}$$

If $\xi(x)$ changes from 0 to s over a distance l and $ql \ll 1$, then a sufficiently weak $U_{\text{eff}}(x)$ can be replaced by $U_0 s\delta(x)$ with

$$U_0 s=\int_{-\infty}^{\infty}dx\ U_{\text{eff}}(x) . \tag{A4}$$

[If $q_0 l \ll 1$, which appears to be satisfied for reasonable values of the parameters, we expect U_{eff} to be sufficiently weak for Eq. (A4) to hold. If not, then Eqs. (17) and (18) still hold for small q, but the relationship of $U_0 s$ to U_{eff} is more complicated than Eq (A4).] The form of T then follows from the continuity of ψ at $x=0$ and the discontinuity in $d\psi/dx$ obtained from integrating (A2) over the singularity at the origin.

If $\xi(x)$ changes abruptly, higher lying states χ_n (with energy E_n), such as the Rydberg series of image states,[22] can be excited virtually. For an abrupt, but small change in $\xi(x)$, it can be shown that

$$T=I_0/(1-q_0/iq) , \tag{A5}$$

where

$$I_0=\int_{-\infty}^{\infty}dz\ \Phi(z-s)\Phi(z) \tag{A6}$$

and

$$q_0=\tfrac{1}{2}\sum_n Q_n I_n^2 , \tag{A7}$$

with

$$Q_n=[2m_n(E_n-E)/\hbar^2]^{1/2} \tag{A8}$$

and

$$I_n=\int_{-\infty}^{\infty}dz\ \Phi(z-s)\chi_n(z) . \tag{A9}$$

Equation (A5) is the same as Eq. (17) except for the factor I_0, which is close to unity for small s and weak energy dependence of Q_n. Thus, we expect that Eq. (17) is an adequate approximation for T.

The nature of the potential near a step on the surface of a jellium metal has been discussed by Thompson and Huntington.[17,18] The principal feature is a small dipole potential localized at the step, which is responsible for the lowering of the work function where there is an appreciable density of steps.[18] If the electron follows a smooth contour that goes up (or down) the step, it should see regions of both positive and negative potential (relative to the flat surface) due to the dipole. From the work of Ref. 17, it appears that this potential variation is small. Thus the dominant factors in the effective barrier potential are the kinematic effects discussed above.

Finally, it should be mentioned that this analysis superficially resembles effective range expansions in three-dimensional scattering theory.[23] Because of the differences between one and three dimensions, however, it is difficult to make a direct comparison. In three dimensions, the strength of the scattering (cross section at zero energy) is determined by a scattering length, whereas in the present case, the measure of the barrier potential strength, q_0, has dimensions of inverse length.

[1]W. J. Kaiser and R. C. Jaklevic, Surf. Sci. **182**, L227 (1987).
[2]R. C. Jaklevic and L. Elie, Phys. Rev. Lett. **60**, 120 (1988).
[3]W. J. Kaiser and R. C. Jaklevic, IBM J. Res. Develop. **30**, 411 (1986).
[4]R. J. Hamers, R. M. Tromp, and J. E. Demuth, Phys. Rev. Lett. **56**, 1972 (1986).
[5]M. P. Everson, R. C. Jaklevic, and W. Shen, J. Vac. Sci. Technol. A **8**, 3662 (1990).
[6]S. D. Kevan and R. H. Gaylord, Phys. Rev. B **36**, 5809 (1987).
[7]M. P. Everson, L. C. Davis, R. C. Jaklevic, and W. Shen, J. Vac. Sci. Technol. (to be published).
[8]D. M. Zeher and J. F. Wendelken, *Proceedings of the Seventh International Vacuum Congress on Solid Surfaces, Vienna, 1977,* edited by R. Dobrozemsky *et al.* (Berger, Vienna, 1977), p. 517. For recent STM work on the reconstruction, see Ch. Wöll, S. Chiang, R. J. Wilson, and P. H. Lippel, Phys. Rev. B **39**, 7988 (1989).
[9]J. Tersoff and D. R. Hamann, Phys. Rev. B **31**, 805 (1985).
[10]J. Bardeen, Phys. Rev. Lett. **6**, 57 (1961).
[11]J. Tersoff, Phys. Rev. B **41**, 1235 (1990).
[12]A. A. Lucas, H. Morawitz, G. R. Henry, J.-P. Vigneron, Ph. Lambin, P. H. Cutler, and T. E. Feuchtwang, J. Vac. Sci. Technol. A **6**, 296 (1988).
[13]N. D. Lang, Phys. Rev. Lett. **55**, 230 (1985).
[14]N. D. Lang, Phys. Rev. Lett. **56**, 1164 (1986).
[15]C. J. Chen, J. Vac. Sci. Technol. A **6**, 319 (1988).
[16]A. Modinos, G. C. Aers, and B. V. Paranjape, Phys. Rev. B **19**, 3996 (1979).
[17]M. D. Thompson and H. B. Huntington, Surf. Sci. **116**, 522 (1982).
[18]A. Zangwill, *Physics at Surfaces* (Cambridge University, Cambridge and New York, 1988).
[19]R. E. Borland, Proc. Phys. Soc. London **78**, 314 (1961).
[20]P. Knipp, Phys. Rev. B **40**, 7993 (1989).
[21]A. P. Shapiro, T. Miller, and T.-C. Chiang, Phys. Rev. B **38**, 1779 (1990).
[22]D. Straub and F. J. Himpsel, Phys. Rev. B **33**, 2256 (1986).
[23]N. F. Mott and H. S. W. Massey, *The Theory of Atomic Collisions* (Clarendon, Oxford, 1965).